Anyon delocalization transitions out of a disordered fractional quantum anomalous Hall insulator

PNAS RESEARCH ARTICLE | PHYSICS

Anyon delocalization transitions out of a disordered fractional quantum anomalous Hall insulator

Zhengyan Darius Shi[a,1] and T. Senthil[a,1]

Affiliations are included on p. 8.

Contributed by T. Senthil; received July 29, 2025; accepted November 3, 2025; reviewed by Jason Alicea and S. A. Parameswaran

Motivated by the experimental discovery of the fractional quantum anomalous Hall effect, we develop a theory of doping-induced transitions out of the $\nu = 2/3$ lattice Jain state in the presence of quenched disorder. We show that disorder strongly affects the evolution into the conducting phases described in our previous work. The delocalization of charge $2/3$ anyons leads to a chiral superconductor through a direct second-order transition for a smooth random potential with long-wavelength modulations. The longitudinal resistance has a universal peak at the associated quantum critical point. Close to the transition, we show that the superconducting ground state is an "Anomalous Vortex Glass" stabilized in the absence of an external magnetic field. For short-wavelength disorder, this transition generically splits into three distinct ones with intermediate insulating topological phases. If instead, the charge $1/3$ anyon delocalizes, then at low doping the resulting phase is a Reentrant Integer Quantum Hall state with $\rho_{xy} = h/e^2$. At higher doping this undergoes a second transition to a Fermi liquid metal. We show that this framework provides a plausible explanation for the complex phase diagram recently observed in twisted $MoTe_2$ near $\nu = 2/3$ and discuss future experiments that can test our theory in more detail.

superconductivity | quantum Hall | anyons | correlated electrons | moire materials

Significance

Fractional quantum anomalous Hall (FQAH) insulators are a class of topological phases realized at zero magnetic field in two-dimensional electronic systems. A distinguishing property of FQAH insulators is the emergence of dispersive anyon excitations with fractional charge and statistics. Doping FQAH insulators nucleates a nonzero density of anyons. While disorder localizes anyons at low doping, increasing the dopant density drives a continuous transition into a chiral superconductor. Remarkably, across the transition, localized anyons transmute into spontaneous vortices in the superconductor, creating an unconventional "anomalous vortex glass" phase. Our theory provides a possible phenomenological account of the complex phase diagram in twisted $MoTe_2$ and reveals a rich interplay between disorder and anyon-induced superconductivity in the doped FQAH regime.

The discovery of zero-field fractional quantum anomalous Hall (FQAH) phases in twisted $MoTe_2$ ($tMoTe_2$) and rhombohedral graphene (1–6) opens up a new frontier in topological materials research. In common with conventional fractional quantum Hall (FQH) phases stabilized in a large external magnetic field (7), FQAH phases host anyon excitations with fractional charge and fractional statistics (8–12). However, unlike in the large-field setting, anyons in FQAH phases are not confined to cyclotron orbits and carry a nontrivial band dispersion. Moreover, the two-dimensional Van der Waals materials that realize FQAH phases come with additional tuning knobs such as the displacement field, which allow for a continuous modulation of the anyon dispersion. This tunability enables us to explore the interplay between topology, electron kinetic energy, and interactions.

The existence of nontrivial anyon dispersion has a profound impact on the fate of FQAH phases upon doping. In the large-field setting, anyons doped into the system carry no kinetic energy and become localized in the presence of disorder (see ref. 13 and references therein). This mechanism explains the formation of quantum Hall plateaus which persist until the basic physics responsible for the emergence of anyons is destroyed. In contrast, the kinetic energy of anyons doped into an FQAH insulator competes with the disorder-induced tendency toward localization. This competition decreases the width of plateau regions and favors the formation of itinerant anyonic quantum phases upon exiting the plateau.

Recent theoretical works have explored the doped FQAH regime in an ideal limit with no disorder (14–16), uncovering a variety of interesting phases including topological superconductors* and charge-ordered Fermi (and non-Fermi) liquids. Subsequently, an experiment in $tMoTe_2$ indeed finds a narrow plateau around the Jain state at lattice filling $\nu = 2/3$ and a superconductor that emerges at $\nu > 2/3$ outside the plateau region (22). On the opposite side $\nu < 2/3$, a reentrant integer quantum anomalous Hall (RIQAH) state apparently arises in between the plateaus surrounding $\nu = 2/3$ and $\nu = 3/5$. This rich phenomenology contrasts with the sequence of FQH plateau transitions that

*The notion of superconductivity developing in a mobile gas of anyons—dubbed "anyon superconductivity"—is an old idea (17–20) that has been refined and extended recently (14, 21). We caution that the superconducting state itself has universal properties that are the same as an electronic superconductor and need not have any anyon excitations. Thus a better terminology is to refer to the superconductor stabilized in a mobile anyon fluid as "anyon-induced superconductivity."

Author contributions: T.S. designed research; Z.D.S. and T.S. performed research; and Z.D.S. and T.S. wrote the paper.

Reviewers: J.A., California Institute of Technology; and S.A.P., University of Oxford.

The authors declare no competing interest.

[1]To whom correspondence may be addressed. Email: zhengyanshinj@gmail.com or senthil@mit.edu.

This article contains supporting information online at https://www.pnas.org/lookup/suppl/doi:10.1073/pnas.2520608122/-/DCSupplemental.

Published December 19, 2025.

occur in the conventional quantum Hall setting within the same range of Landau level filling (7, 23).

Motivated by these experimental discoveries, we focus on the lattice Jain state at filling $\nu = 2/3$ and study its evolution into the conducting states described in our previous work (14). First, we study the chemical potential tuned FQAH-SC phase transition in both the clean and dirty limits (see Fig. 1 for a representation of this transition in terms of flux-attached nonrelativistic fermions). We also discuss a bandwidth tuned FQAH-SC transition at fixed lattice filling $\nu = 2/3$. Our analysis of the dirty limit shows that quenched disorder modifies the FQAH-SC evolution in striking ways that we elaborate on below. Second, we also analyze the chemical potential tuned evolution from the FQAH state to a charge-ordered Fermi liquid metal (also obtained in our previous work). In the presence of disorder, while the details of the evolution are complicated, the charge-ordered metal is replaced by an integer quantum Hall state in a portion of the phase diagram.

The main characters in our analysis are a pair of basic anyonic excitations of the Jain state, $a_{1/3}$ and $a_{2/3}$, which carry fractional charges $e/3$ and $2e/3$ respectively. The possible doping-induced phases as well as the universality class of phase transitions between them depend sensitively on the energetics of $a_{1/3}$ and $a_{2/3}$ in the undoped Jain state. When the energy gap of $a_{2/3}$ is smaller than twice the energy gap of $a_{1/3}$, the doped charges enter as a fluid of $a_{2/3}$ anyons.[†] At low dopant density, disorder turns this fluid into a localized anyon glass. For a smooth disorder potential with only long-wavelength modulations, increasing doping induces a direct continuous transition into a chiral superconductor. The longitudinal resistance has a universal peak of $\mathcal{O}(h/e^2)$ at the $T = 0$ quantum critical point, which is broadened at nonzero temperatures (Figs. 2 and 3). We argue that localized anyons in the anyon glass phase evolve into an "Anomalous Vortex Glass" (AVG) in the superconductor sufficiently close to the critical point. The finite-temperature dynamics of this phase share many features with the field-induced vortex glass (26, 27) in conventional type-II superconductors. In particular, vortex creep destabilizes the AVG SC at $T > 0$, resulting in a finite resistivity and nonlinear current-voltage characteristics at low current densities. With short-wavelength disorder (e.g. from point defects), a direct FQAH-SC transition is forbidden and the system instead passes through two intermediate phases with quantized electrical and thermal transport (Fig. 4). The critical points between these phases have similarities with plateau transitions between FQH phases that we will comment on below.

When the energy gap of a localized $a_{2/3}$ anyon is larger than twice the energy gap of $a_{1/3}$, the dopant charges form a fluid of $a_{1/3}$ anyons instead. In this case, with both short and long-wavelength disorder, we argue that there is a direct transition from the anyon glass at low doping to an integer quantum Hall (IQH) state with $\sigma^{xy} = e^2/h$ at higher doping (Fig. 5).

The theory developed above applies to any doped lattice $\nu = 2/3$ Jain state. The main input from microscopics is the relative gap sizes of distinct anyons which determine whether $a_{1/3}$ or $a_{2/3}$ is doped into the system.[‡] Armed with our theoretical analysis, we discuss the observation of SC and RIQAH states proximate to the $\nu = 2/3$ FQAH state in tMoTe$_2$. We propose an interpretation of the tMoTe$_2$ phase diagram from ref. 22, in which doping toward $|\nu| > 2/3$ induces a fluid of $a_{2/3}$ anyons, while doping toward $|\nu| < 2/3$ induces a fluid of $\bar{a}_{1/3}$ anyonic holes. This asymmetry in the particle and hole excitation spectrum leads to an asymmetric phase diagram in which $\nu > 2/3$ realizes a superconductor while $\nu < 2/3$ realizes a localized IQH state.

Low Energy Theory Near $\nu = 2/3$

Following ref. 14, we describe the Jain state at lattice filling $\nu = 2/3$ through a parton construction in which the microscopic electron c is fractionalized as $c = f_1 f_2 f_3$. The Hilbert space generated by f_i is redundant. In order to project to the physical Hilbert space, we introduce a pair of emergent $U(1)$ gauge fields a, b that couple to the f_i partons through the following low energy Lagrangian

$$L = L[f_1, a] + L[f_2, b - a] + L[f_3, A - b] + \dots , \qquad [1]$$

where each term describes a fermionic band minimally coupled to a $U(1)$ gauge field, and ... denotes interaction terms compatible with gauge-invariance and lattice symmetries

$$L[f, a] = f^\dagger \left[i\partial_t + a_t - \epsilon(i\nabla + \boldsymbol{a}) \right] f + \dots . \qquad [2]$$

The equations of motion for a_t and b_t enforce the constraint $\rho_1 = \rho_2 = \rho_3 = \rho_c$, where ρ_i/ρ_c is the charge density of f_i/c respectively. Throughout the paper, we work in units where the lattice constant is set to 1.

To construct the Jain state at lattice filling $\nu = 2/3$, consider a uniform mean-field ansatz in which

$$\frac{\langle \nabla \times \boldsymbol{a} \rangle}{2\pi} = -\frac{1}{3}, \quad \frac{\langle \nabla \times \boldsymbol{b} \rangle}{2\pi} = \frac{1}{3}. \qquad [3]$$

This choice ensures that the flux seen by f_i is commensurate with its lattice filling $\nu_i = 2/3$. Therefore, each f_i can form a Chern insulator with total Chern number C_i determined by the detailed band structure. The unique Chern number assignment (up to permutations) that reproduces the Jain topological order is $C_1 = -2$, $C_2 = C_3 = 1$ (14). With this choice, we can integrate out the gapped partons f_i as well as the gauge field a to obtain

$$L = \frac{3}{4\pi} b db - \frac{1}{2\pi} b dA + \frac{1}{4\pi} A dA + 2\mathrm{CS}_g . \qquad [4]$$

In the above continuum effective theory, we have included a coupling to the background space-time metric g. The gravitational Chern–Simons term $2\mathrm{CS}_g$ enables us to keep track of the thermal Hall conductance of various phases.

Upon doping away from $\nu = 2/3$, the excess charges form a dilute itinerant anyon fluid. The key observation in ref. 14 is that the fate of this anyon fluid at zero temperature depends on the energetics of different anyons in the parent FQAH insulator. In the parton description, the $a_{1/3}$ anyon is sourced by f_1 (the zero-field analogue of the composite fermion) and the $a_{2/3}$ anyon is sourced by f_2 or f_3. Therefore, the question of which anyon gets doped into the system translates to the question of which parton band is closest to the chemical potential. We now consider both possibilities (doping in $a_{2/3}$ or $a_{1/3}$) and analyze the evolution out of the FQAH phase with and without quenched disorder.

Doping the $a_{2/3}$ Anyon: Clean Limit

Let us first study the situation in which the $a_{2/3}$ anyon is doped into the system. In the absence of disorder, the phase transition

[†] See refs. 24 and 25 for very recent calculations demonstrating bunching of anyons in a Landau level.

[‡] If the electron gap is smaller than three times the $a_{1/3}$ gap, the dopant charges may enter as ordinary electrons instead. If that is the case, the doped electrons naturally form a Fermi liquid that coexists with the background topological order (14), realizing an exotic FL* state (28, 29). We will comment on this possibility in *Discussion*.

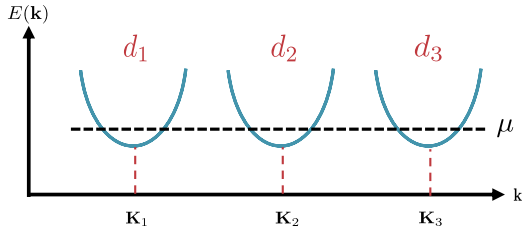

Fig. 1. A schematic depiction of the continuum fields d_I that create excitations of the f_3 band near its minima $\boldsymbol{K}_1, \boldsymbol{K}_2, \boldsymbol{K}_3$. When μ is Above the band bottom, the d_I particles see an emergent magnetic field proportional to their density, which is not shown in the figure.

out of the FQAH state occurs (within the parton description) when the chemical potential μ touches the minima of the unfilled f_3 band. Lattice translations T_x, T_y act projectively on f_3 as it sees $2\pi/3$ flux per plaquette. Thus f_3 carries well-defined crystal momenta in a three-fold reduced Brillouin zone, and its band structure has three degenerate minima at $\boldsymbol{K}_1, \boldsymbol{K}_2, \boldsymbol{K}_3$ such that $|\boldsymbol{K}_I - \boldsymbol{K}_J|$ is a multiple of $2\pi/3$. Importantly, while the location of $\boldsymbol{K}_i$ is gauge-dependent, the differences $\boldsymbol{K}_I - \boldsymbol{K}_J$ are gauge-invariant and physical. Near the critical point, it is convenient to introduce three species of continuum fermionic fields d_I that create f_3 excitations near $\boldsymbol{K}_I$ and transform projectively under lattice translation (see Fig. 1 for an illustration)

$$T_x : d_I \to d_{I+1}\,, \quad T_y : d_I \to e^{2\pi i I/3} d_I\,. \tag{5}$$

In terms of these fields, the low energy effective Lagrangian takes the form

$$\begin{aligned} &L_{\text{clean},a_{2/3}} \\ &= \sum_{I=1}^{3} d_I^\dagger \left[i\partial_t + \mu + A_t - b_t - \frac{(i\nabla + \boldsymbol{A} - \boldsymbol{b})^2}{2m} \right] d_I \\ &\quad + L_{\text{int}}[d_I] + \frac{3}{4\pi} bdb - \frac{1}{2\pi} bdA + \frac{1}{4\pi} AdA + 2\text{CS}_g\,, \end{aligned} \tag{6}$$

where m is the effective mass of f_3 near the band minima and L_{int} includes repulsive interactions between the d_I fermions. When $\mu < 0$, the d_I fermions are gapped and we recover the Jain state described by Eq. **4**. When $\mu > 0$, the equations of motion for b_t enforce the constraint $\sum_{I=1}^{3} \rho_I = \frac{3}{2\pi} \langle \nabla \times \boldsymbol{b} \rangle$. Since d_I feels an effective magnetic field $-\nabla \times \boldsymbol{b}$, this constraint implies that each d_I is at Landau level filling -1 and forms an IQH state. Integrating out the filled Landau levels of d_I gives the chiral topological charge-2 superconductor

$$L_{\text{SC}} = \frac{2}{2\pi} bdA - \frac{2}{4\pi} AdA - 4\text{CS}_g\,. \tag{7}$$

It is natural to wonder how the expected $h/2e$ flux quantization works out in this superconductor given its origins from a fluid of charge-2/3 anyons. We show in *SI Appendix*, section 2 that if we start with an annulus in the FQAH phase with an $a_{2/3}$ anyon trapped in the inner hole, then upon transitioning to the SC, a vorticity of $-2\pi \mod 6\pi$ in the phase of the Cooper pair order parameter is induced (corresponding to quantized flux $-h/2e \mod 3h/2e$). If instead an $a_{1/3}$ anyon is initially trapped in the inner hole, then a Cooper pair vorticity of $+2\pi \mod 6\pi$ is induced in the SC. The general phenomenon of anyons transmuting into vortices is well known (30, 31) in SC arising in, e.g., doped Z_2 spin liquid Mott insulators though the details, such as the 6π periodicity and the asymmetry between $\pm 2\pi$ vortices, are different in the present context.

At the critical point $\mu = 0$, the mean-field propagator for d_I takes the simple form

$$G_{IJ}^{(d)}(\boldsymbol{k}, i\omega) = \frac{\delta_{IJ}}{i\omega - k^2/(2m)}\,. \tag{8}$$

As a result, the dynamical critical exponent is $z = 2$ and the correlation length exponent is $\bar{\nu} = 1/2$. A short-range interaction of the form $V_{IJ}\rho_I\rho_J$ is marginal at tree level. Following the same calculation as in the Bose-Hubbard model (32), we can show that V_{IJ} is marginally irrelevant and can be neglected at the IR fixed point.

The interaction between d_I and the gauge field b is also marginal by power counting. Nevertheless, we can argue that the gauge and matter sectors decouple at zero temperature. The physical reason is that the dispersion of d_I contains a "particle" branch above μ but no hole branch below μ. This means that the ground state contains no occupied fermionic modes and particle–hole excitations do not exist at zero temperature. Since the gauge field b couples to particle–hole excitations, this observation immediately implies the decoupling between matter and gauge sectors at $T = 0$. On a more technical level, this is equivalent to the statement that poles of $G_{IJ}^{(d)}(\boldsymbol{k}, i\omega)$ in the complex ω-plane always satisfy $\text{Im}[\omega] < 0$. This pole structure guarantees that all loop corrections to the gauge field self-energy vanish identically.

Doping the $a_{2/3}$ Anyon: Dirty Limit

For real experimental systems, quenched disorder is ubiquitous and modifies the above picture dramatically. The most relevant form of disorder near the phase transition is a generalized random potential that breaks the lattice translation symmetry completely

$$L_{\text{dis}} = W_{IJ}(\boldsymbol{r}) d_I^\dagger(\boldsymbol{r}, t) d_J(\boldsymbol{r}, t) + W_b(\boldsymbol{r}) \frac{\nabla \times \boldsymbol{b}(\boldsymbol{r}, t)}{2\pi}\,. \tag{9}$$

When μ is positive but small, each of the d_I fermions wants to form an IQH state with a small energy gap $\omega_c(\delta) \sim \delta/m$, where $\delta \ll 1$ is the density of d_I. Let $\overline{W}_{IJ}$, $\overline{W}_b$ characterize the strength of the disorder potentials $W_{IJ}(\boldsymbol{r})$, $W_b(\boldsymbol{r})$. If $\omega_c(\delta) \ll \overline{W}_{IJ}, \overline{W}_b$, the mean-field quantum Hall state for d_I is replaced by a localized state with vanishing σ^{xx} and σ^{xy}. Gauge fluctuations turn this mean-field state into a localized "anyon glass," leading to a plateau surrounding the $\nu = 2/3$ state with quantized $\sigma^{xy} = 2e^2/3h$. In the opposite limit where $\omega_c(\delta) \gg \overline{W}_{IJ}, \overline{W}_b$, the disorder potential is a weak perturbation to the mean-field IQH state of d_I and we recover a disordered superconductor.

The evolution from the anyon glass to the superconductor depends on the spatial profile of the disorder potentials. In what follows, we will consider the smooth limit, in which $W_{IJ}(\boldsymbol{r})/W_b(\boldsymbol{r})$ only contains long-wavelength modulations, and the rough limit, in which $W_{IJ}(\boldsymbol{r})/W_b(\boldsymbol{r})$ has significant fluctuations on the lattice scale. These two limits lead to drastically different phase diagrams, as we now explain.

Smooth Random Potentials. When $W_{IJ}(\boldsymbol{r})/W_b(\boldsymbol{r})$ is a smooth potential with only long-wavelength modulations, we can truncate the Fourier modes $W_{IJ}(\boldsymbol{q})/W_b(\boldsymbol{q})$ at some small momentum cutoff $q_{\max} \ll 1$ (in units where the lattice spacing is 1). In the low energy effective theory, this means that disorder potentials that transform under the action of lattice translations should be

excluded. From Eq. **5**, it is clear that $d_I^\dagger V_{IJ} d_J$, with V_{IJ} any $SU(3)$ matrix, transforms nontrivially under T_x and/or T_y. Therefore, the only terms compatible with smooth disorder take the form

$$L_{\text{dis,smooth}} = W_d(\boldsymbol{r}) \sum_{I=1}^{3} d_I^\dagger d_I + W_b(\boldsymbol{r}) \frac{\nabla \times \boldsymbol{b}(\boldsymbol{r})}{2\pi} . \qquad [10]$$

When $L_{\text{dis,smooth}}$ is added to the critical theory, the combined Lagrangian enjoys an emergent $SU(3)$ symmetry[§] that rotates the fermionic fields d_I. As we increase the dopant density δ (by tuning the chemical potential μ), there is a critical δ_{c1} (μ_{c1}) at which d_I goes through an $SU(3)$-symmetric plateau transition with a jump in the Hall conductance $\Delta\sigma_d^{xy} = -3e^2/h$. With gauge fluctuations, this turns into a direct transition from the anyon glass (with quantized $\sigma^{xy} = 2e^2/3h$) to a chiral superconductor with $R^{xx} = R^{xy} = 0$ at $T = 0$.

At first glance, one may expect Eq. **7** to capture the universal properties of the superconductor close to the phase transition. However, this expectation turns out to be incorrect due to subtle localization effects. Below the critical chemical potential μ_{c1}, the doped anyons completely localize at zero temperature. Within the effective field theory, these localized anyons are described as localized d_I fermions attached to gauge fluxes of b. Across $\mu = \mu_{c1}$, a small fraction of the d_I particles delocalize and drive the Hall conductance jump $\Delta\sigma_d^{xy} = -3e^2/h$. The key question is: what happens to the localized anyons once the delocalized anyons form a superconducting condensate? As we argue in *SI Appendix*, section 2, sufficiently close to the transition, these localized anyons in the anyon glass phase evolve into a nonzero density of randomly pinned vortices of strength either $-h/2e$ or h/e in the superconductor, with vanishing total vorticity. Since these vortices emerge at zero external magnetic field and exhibit glassy dynamics (26, 27), we refer to this many-body state as an "Anomalous Vortex Glass" (AVG) superconductor. This phase is characterized by a nonvanishing Edwards-Anderson superconducting order parameter. Like the field-induced vortex glass, the AVG is not stable to thermal fluctuations at $T > 0$ due to the creep motion of vortices. As a result, the linear resistance is nonzero at any $T > 0$. Furthermore the current-voltage characteristics exhibit nonlinearities at a low current density scale $J_T \sim T^{1+\frac{1}{|\theta|}}$ with θ a universal exponent estimated (33) to be around 0.5. There is thus no sharp finite-temperature phase transition at small $\mu - \mu_{c1}$.

Upon increasing μ, the density of vortices gradually decreases and vanishes at a second critical point $\mu_{c2} > \mu_{c1}$. Dissipationless transport is restored at $T > 0$ for $\mu > \mu_{c2}$ and the finite-temperature transition out of this SC state belongs to the standard Berezinsky–Kosterlitz–Thouless (BKT) universality class.

While the precise critical exponents of the transitions at μ_{c1} and μ_{c2} are difficult to access analytically, there are a number of qualitative features that can be immediately deduced. Within the parton description, the d_I fermions are gapless but not gauge-invariant. The gauge-invariant electron operator c can be constructed by combining d_I with the gapped partons f_1 and f_2. Therefore, the microscopic electron remains gapped across the FQAH-SC evolution and single particle tunneling sees no spectral weight at frequencies below the f_1/f_2 gap. This may also be understood more generally as, by assumption, the $a_{1/3}$ gap stays nonzero across the evolution into the SC, and it is not possible to build the electron by fusing powers of $a_{2/3}$ alone.

[§] More precisely, the symmetry is $PSU(3) = SU(3)/\mathbb{Z}_3$.

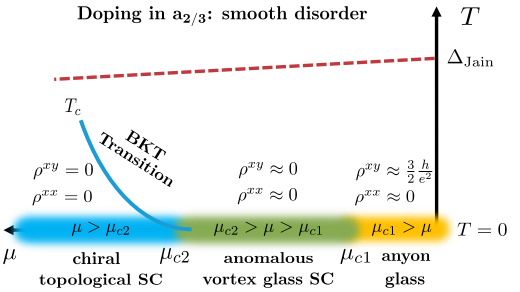

Fig. 2. Onset of T_c and ρ_S as a function of μ across the FQAH-SC evolution with smooth disorder. In this phase diagram, we assume that μ is close enough to the chemical potential of the parent FQAH insulator so that the Jain gap Δ_{Jain} remains much higher than T_c. The anomalous vortex glass (AVG) SC and the chiral topological SC both have zero resistance at $T = 0$. At $T > 0$, the AVG has a small nonzero resistance due to the creep motion of vortices. As a result, there is no sharp finite-temperature phase transition into the AVG and $T_c = 0$ for $\mu_{c2} > \mu > \mu_{c1}$. While ρ^{xx} and ρ^{xy} show variable range hopping transport in the anyon glass, they show power-law temperature dependence in the AVG phase due to thermal creep of vortex configurations.

In terms of transport, general scaling arguments imply that the critical theory at μ_{c1} has a universal nonzero resistivity tensor ρ_c with both longitudinal and Hall components of $\mathcal{O}(h/e^2)$ (32, 34–36). This may be approximately related to the conductivity tensor σ_d of d_I through the Ioffe-Larkin rule

$$\rho_c = \begin{pmatrix} 0 & -1/2 \\ 1/2 & 0 \end{pmatrix} + \left[\begin{pmatrix} 0 & 1 \\ -1 & 0 \end{pmatrix} + \sigma_d \right]^{-1} . \qquad [11]$$

Computing the inverse explicitly gives

$$\rho_c^{xx} = \frac{\sigma_d^{xx}}{(\sigma_d^{xx})^2 + (1+\sigma_d^{xy})^2} ,$$
$$\rho_c^{yx} = \frac{1}{2} + \frac{1+\sigma_d^{xy}}{(\sigma_d^{xx})^2 + (1+\sigma_d^{xy})^2} . \qquad [12]$$

Thus the critical point is signaled by a universal peak in ρ^{xx}. At $T > 0$, the peak is broadened by thermal fluctuations, with a width that scales as $T^{1/(\bar{\nu}z)}$. The critical exponents $\bar{\nu}, z$ are constrained by standard arguments (32, 37) for disordered superfluid–insulator transitions. With short-range interactions, both phases as well as the critical point are compressible and this implies an exact dynamical critical exponent $z = 2$. (With Coulomb interactions, z is modified to 1). Moreover, by the Harris-Chayes bound (38, 39), the correlation length exponent $\bar{\nu}$ satisfies the inequality $\bar{\nu} \geq 1$ in two dimensions. As a result, $\bar{\nu}z \geq 2$ and the width of the resistance peak shrinks as a slow power law of T.

For $\mu_{c1} < \mu < \mu_{c2}$, the AVG phase has a nonvanishing resistance at $T > 0$ that gradually decreases to zero as μ approaches the second transition at μ_{c2}. If the localized anyon density is small at $\mu = \mu_{c1}$, the AVG phase occupies a very narrow region on the μ-axis and an apparent direct transition between the FQAH anyon glass and the ordinary SC would occur at moderate temperature. In that case, the scaling of $\rho_s(\mu)$ follows an approximate scaling form

$$\rho_s \sim \xi^{-z} \sim |\mu - \mu_{c1}|^{\bar{\nu}z} . \qquad [13]$$

This phenomenology is summarized in Figs. 2 and 3.

Rough Random Potentials. The story is drastically different when the microscopic disorder potentials $W_{IJ}(\boldsymbol{r})$ and $W_b(\boldsymbol{r})$

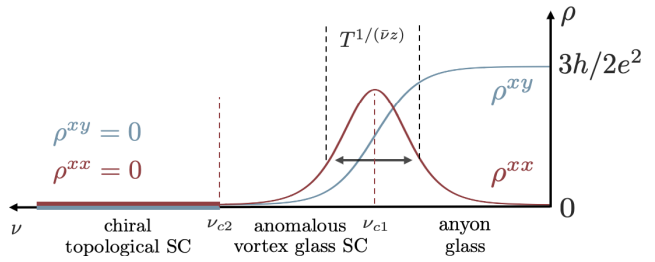

Fig. 3. Evolution of ρ upon doping $a_{2/3}$ at fixed $T > 0$ with smooth disorder. To match the experimental convention, our plot shows ν increasing toward the *Left*. ν_{c1} marks the $T = 0$ critical point with universal transport and ν_{c2} defines the transition from the AVG to the chiral topological SC. Whether the chiral topological SC can be observed in experiment depends on the width of the AVG region, which requires a more detailed microscopic calculation.

have significant variations at the lattice scale. In this case, all components of W_{IJ} must be included and the emergent $SU(3)$ symmetry in the clean Lagrangian is completely broken. As δ increases, the evolution from $\sigma_d^{xy} = 0$ to $\sigma_d^{xy} = -3$ passes through three separate phase transitions, as σ_d^{xy} can only jump by ± 1 at each critical point. When $\sigma_d^{xy} = -1$, the effective Lagrangian reduces to

$$L[\sigma_d^{xy} = -1] = \frac{2}{4\pi} bdb\,, \qquad [14]$$

which describes a localized insulator that coexists with a neutral $U(1)_{-2}$ topological order. This phase is indistinguishable from a trivial localized insulator in electric transport but has a single neutral chiral edge mode with $\kappa_{xy} = -2\kappa_Q$ that can potentially be detected in thermal Hall measurements.[¶] When $\sigma_d^{xy} = -2$, the effective Lagrangian becomes

$$L[\sigma_d^{xy} = -2] = \frac{1}{4\pi} bdb + \frac{1}{2\pi} bdA - \frac{1}{4\pi} AdA - 2\mathrm{CS}_g\,. \qquad [15]$$

Integrating out b simplifies this Lagrangian further to

$$L[\sigma_d^{xy} = -2] = -\frac{2}{4\pi} AdA - 4\mathrm{CS}_g\,, \qquad [16]$$

which describes an IQH state with Hall conductance $\sigma^{xy} = -2$. Putting all of these results together, we arrive at the phase diagram in Fig. 4, where each critical point is associated with a universal $\mathcal{O}(h/e^2)$ resistivity tensor. At $T > 0$, the width of the transition region scales as $T^{1/(\bar{\nu}z)}$, while the critical resistivity is independent of T. Importantly, although the three critical points involve the same jump in σ_d^{xy} at the mean field level, they differ in the structure of gauge interactions and could have distinct critical exponents. If we decrease the disorder strength at fixed T, the range of δ over which the three transitions occur shrinks and the peaks eventually merge into a smoother evolution of ρ^{xx} and ρ^{yx}.

Doping the $a_{1/3}$ Anyon

We now turn to the second possibility, in which the doped anyon is $a_{1/3}$ and the f_1 band is closest to the chemical potential. In the clean limit, we again introduce three species of d_I that create excitations of f_1 near its band minima at $\boldsymbol{K}_I$ such that d_I transforms projectively under T_x, T_y as in Eq. **5**. The low energy effective Lagrangian then takes the form

$$L_{\mathrm{clean},a_{1/3}} = \sum_{I=1}^{3} d_I^\dagger \left[i\partial_t + \mu + a_t - \frac{(i\nabla + \boldsymbol{a})^2}{2m} \right] d_I + L_{\mathrm{int}}[d_I] - \frac{1}{4\pi} ada + \frac{2}{4\pi} bdb + \frac{1}{4\pi} AdA - \frac{1}{2\pi} bd(A+a)\,, \qquad [17]$$

where m now denotes the effective mass of f_1 near the band minima. When $\mu < 0$, d_I is gapped and we recover the Jain state. When $\mu > 0$, the equations of motion for a_t and b_t enforce the constraint $\sum_I \rho_I = \frac{3}{2}\frac{1}{2\pi}\langle \nabla \times \boldsymbol{a} \rangle$. At the mean-field level, each d_I feels an effective magnetic field $\nabla \times \boldsymbol{a}$ and is at Landau level filling 1/2. Therefore, the three species of d_I form three pockets of composite Fermi liquids coupled to a common fluctuating gauge field a. The analysis in ref. 14 shows that gauge fluctuations induce interpocket pairing between two out of the three pockets and confine all the fluctuating gauge fields. The resulting ground state is a charge-ordered Fermi liquid coexisting with a background IQH state

$$L_{\mathrm{FL}} = L_{\mathrm{FL}}[c, A] + \frac{1}{4\pi} AdA + 2\mathrm{CS}_g\,. \qquad [18]$$

The clean critical theory is identical to the clean FQAH-SC transition at the mean field level and the argument for decoupling between gauge and matter sectors still holds at $T = 0$. At $T > 0$, this transition differs from the FQAH-SC transition since the relevant gauge fields have different Chern–Simons terms. A quantitative understanding of these finite-temperature properties is an interesting target for future studies.

The story has an interesting twist when we include quenched disorder. With long-wavelength disorder, the random potential Lagrangian still takes the $SU(3)$ symmetric form in Eq. **10**. At low doping, the resulting state is an anyon glass (with quantized $\sigma^{xy} = 2e^2/3h$) made of $a_{1/3}$ instead of $a_{2/3}$. Unlike in the FQAH-SC case, the mean-field transition is not an IQH plateau transition of d_I. Instead, it describes the creation of three composite fermion pockets out of a localized insulator, about which very little is understood. Moreover, on the other side of the phase transition, the Fermi liquid with period-3 charge order predicted by the clean theory will not be stable to localization effects at low doping density. In the resulting state, the $L_{\mathrm{FL}}[c, A]$ part of Eq. **18** becomes a Fermi glass and the theory describes an IQH state with quantized $\sigma^{xx} = 0$ and $\sigma^{xy} = e^2/h$. Under the approximation that the smooth disorder potential does not couple linearly to the CDW order parameter, the charge order will survive in this IQH state.

With short-wavelength disorder, the random potential breaks the $SU(3)$ symmetry. At finite doping, the charge order of the doped Fermi liquid will be unstable to disorder. As before at

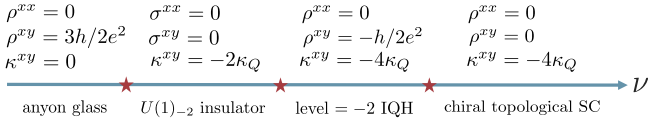

Fig. 4. With short-wavelength disorder, the FQAH-SC evolution passes through three intermediate phases with quantized ρ and κ^{xy}. In the phase diagram *Above*, $U(1)_{-2}$ is a neutral topological order and κ_Q denotes the thermal Hall quantum corresponding to a single Majorana edge mode.

[¶] This state can also be obtained by doping the CDW* state with neutral $U(1)_{-2}$ topological order at $\nu = 2/3$ which is accessible from the Jain state through a bandwidth-tuned transition (40).

low doping densities the Fermi liquid will again be unstable to localization. The integer quantum Hall effect of the clean CDW metal will survive. Let us now consider the evolution from the FQAH to this IQH phase. The individual filling factors of d_I are no longer meaningful and we can regard d_I as a three-component fermion at total Landau level filling 3/2. At low doping, d_I forms a localized insulator and we again have an anyon glass of $a_{1/3}$. This of course is part of the FQAH plateau. Upon increasing the doping, it is natural to encounter a plateau transition in which the total Hall conductance of the d_I sector jumps by 1. When this occurs, the effective Lagrangian becomes

$$L = \frac{2}{4\pi} bdb + \frac{1}{4\pi} AdA - \frac{1}{2\pi} bd(A+a) + 2\mathrm{CS}_g \,. \qquad [19]$$

Integrating out a sets $b = 0$ and gives

$$L[\sigma_d^{xy} = 1] = \frac{1}{4\pi} AdA + 2\mathrm{CS}_g \,, \qquad [20]$$

which just describes an IQH state coexisting with a localized Fermi glass. As argued above, this is exactly the fate of the clean CDW metal (+IQH) at low charge densities in the presence of short wavelength disorder.

Therefore, the most natural state that arises from doping in $a_{1/3}$ is always an IQH state with quantized $\sigma^{xy} = e^2/h$, although the nature of the transition from the Jain state to this IQH state could depend on the type of quenched disorder. A schematic transport plot is shown in Fig. 5.

Bandwidth-Tuned FQAH-SC Transition

We now briefly consider the possibility that the FQAH state can be tuned to a SC at fixed lattice filling $\nu = 2/3$ by varying the bandwidth (e.g. with a displacement field) in the clean limit. To that end, we begin with the parton description of the FQAH state in terms of f_i for $i = 1, 2, 3$ each filling a Chern band with Chern numbers C_i such that $C_1 = -2, C_2 = C_3 = 1$. We consider a phase transition at fixed filling where the Chern number of f_3 changes away from 1 (through band inversion) while the f_1, f_2 Chern numbers stay fixed. As we discussed, the projective action of translation symmetry implies that there are three inequivalent points in the Brillouin zone that are degenerate in energy. Consequently, the band touching happens simultaneously at these three points, each described by a massless Dirac fermion. The f_3 Chern number can therefore only jump by multiples of 3 so long as the lattice translation symmetry is preserved.

Consider now a phase where the Chern number of f_3 has changed from its original value $C_3 = 1$ in the FQAH phase to

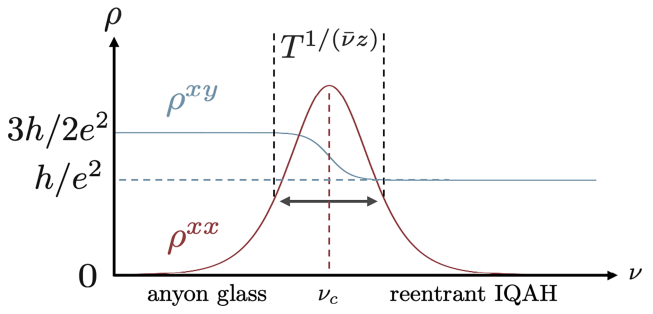

Fig. 5. Evolution of ρ^{xx} and ρ^{xy} upon doping the $a_{1/3}$ anyon. At $\nu > \nu_c$, the inclusion of disorder turns the charge-ordered Fermi liquid in the clean model into a reentrant IQAH state.

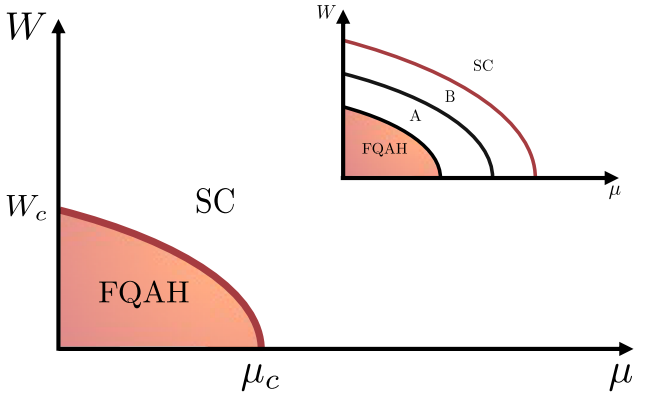

Fig. 6. Schematic phase diagram showing the 2/3 Jain FQAH and chiral topological SC in the bandwidth-chemical potential ($W - \mu$) plane. In a clean system, the phase transition at fixed lattice filling is in a different universality class described by the QED_3-Chern Simons theory of Eq. **22**. With smooth long-wavelength disorder, we expect the AVG phase to appear near the phase boundary, extending from the μ-axis to the W-axis. *Inset*: Dirty limit with short-wavelength disorder. The transition goes through two intermediate phases; phase (A) is an insulator with a neutral topological order and (B) is an integer quantum Hall insulator with $\sigma^{xy} = -2e^2/h$.

$C_3 = -2$. The low energy effective theory of the resulting phase is

$$\begin{aligned} L &= \frac{2}{4\pi} bdb - \frac{2}{4\pi}(A-b)d(A-b) - 4\mathrm{CS}_g \\ &= \frac{2}{2\pi} bdA - \frac{2}{4\pi} AdA - 4\mathrm{CS}_g \,. \end{aligned} \qquad [21]$$

Integrating out b, we see that we get a charge-2 superconductor with a chiral central charge $c_- = -2$, which is smoothly connected to the one obtained by doping the FQAH state with the $a_{2/3}$ anyon Eq. 7. At the mean-field level, the Chern-number-changing transition in the f_3 sector can be described by three massless Dirac fermions. After including gauge fluctuations, the critical Lagrangian takes the form

$$\begin{aligned} L_{\mathrm{Dirac}} = &\sum_{I=1}^{3} d_I^\dagger \left(i\partial\!\!\!/ + A\!\!\!/ - b\!\!\!/\right) d_I \\ &+ \frac{3}{4\pi} bdb - \frac{1}{2\pi} bdA + \frac{1}{4\pi} AdA + 2\mathrm{CS}_g \,. \end{aligned} \qquad [22]$$

This is a QED_3 theory with $N_f = 3$ massless Dirac fermions (representing the 3 band touching points of f_3) coupled to an emergent gauge field $A - b$. As a relativistic theory, it has $z = 1$ and power-law correlations in the CDW order parameters $d_I^\dagger T_{IJ} d_J$ (with T_{IJ} an $SU(3)$ matrix). Its properties are similar to an analogous transition between the bosonic $\nu = 1/2$ Laughlin and superfluid states, which has $N_f = 2$ and distinct Chern–Simons terms. In *SI Appendix*, section 1, we show that a useful perspective on this transition as well as the doping-induced FQAH-SC transition can be obtained by relating them to transitions out of the bosonic Jain state at $\nu = 2/3$.

A schematic phase diagram in the full bandwidth-chemical potential plane is shown in Fig. 6.

Application to Doped *t*$MoTe_2$

A recent experimental study (22) of a high quality hole-doped *t*$MoTe_2$ device explored the phase diagram in the vicinity of the prominent $\nu = 2/3$ FQAH state. In a small range of

displacement field near zero, a SC state is found at fillings $0.71 \lesssim \nu \lesssim 0.76$. This SC is separated from the FQAH state by a region where the longitudinal resistance ρ^{xx} peaks with a peak height of order h/e^2 (in the range 10 to 15 $k\Omega$). On the other side with ν just smaller than 2/3, an integer quantum Hall response is found (dubbed the Rentrant Integer Quantum Anomalous Hall (RIQAH) state) in ρ^{xy} and ρ^{xx}. This too is separated from the FQAH state by a peak in ρ^{xx}. An RIQAH response is also seen at higher displacement field for $\nu \gtrsim 2/3$. Caution is however needed in interpreting the RIQAH response: A plot of the Streda slope in this state yields a σ^{xy} closer to 2/3 than to 1. One possible way to reconcile this discrepancy is to postulate that the apparent RIQAH state is actually a 2/3 state with incomplete equilibration between its two edge components (41–44). This partial equilibration could result in a spurious integer quantization of ρ^{xy}, as observed in experiments. More detailed modeling is needed to assess whether this mechanism accounts for the compressible region in between $\nu = 2/3$ and the filling where an apparent RIQAH state is observed.

It is important for future experiments to resolve this discrepancy between transport and the Streda slopes and to have further confirmation of the superconducting state. We have argued that it is reasonable theoretically to expect both superconductivity and an RIQAH state in proximity to the 2/3 FQAH plateau. Let us therefore examine the existing experimental data in light of our theory.

There are several preliminary questions that need to be settled before interpreting these observations in terms of the theory developed in this paper. For the observed superconductor, it is important to know whether the mobile charge carrier density is "small" (corresponding to filling $2/3 - \nu$, the deviation from 2/3) or if it is "large" (corresponding to filling $1 - \nu$). If the former, then a description as a doped FQAH state—which will naturally involve doped anyons—is the right framework. If the latter, then it is appropriate to think of the SC as developing out of a normal state that is separated from the FQAH state by a strong first-order transition, and the theory described in this paper is not directly pertinent. In both cases, the carrier density can be inferred directly from normal state transport measurements, as sketched in *SI Appendix*, section 3. The existing data reveal a sign change of the Hall effect at high fields $B \gtrsim 2$ T near $\nu \approx 0.75$ at $D = 0$ below which SC first develops. This could be consistent with a "large" to "small" carrier density change, though a more detailed study is needed to determine whether the carrier density truly decreases toward zero as ν approaches 2/3.

Assuming that the doped FQAH framework is applicable, the theory developed so far provides a possible explanation of these observations. At displacement field $D = 0$ and $\nu = 2/3$, we propose that the anyon energetics of the Jain state has a particle–hole asymmetry, such that doping toward $\nu > 2/3$ induces a fluid of $a_{2/3}$, while doping toward $\nu < 2/3$ induces a fluid of $a_{1/3}$. This translates to a parton band structure where the conduction (valence) band closest to the chemical potential is associated with f_3 (f_1). With long-wavelength disorder,[#] there is a narrow plateau with quantized $\sigma^{xy} = 2e^2/3h$ for $\nu \in [\nu_1, \nu_2]$ with $\nu_1 < 2/3 < \nu_2$. Doping beyond the plateau, our theory predicts a topological superconductor at $\nu > \nu_2$ and an RIQAH state at $\nu < \nu_1$. While all three phases have $\rho^{xx} = 0$, the transitions between them feature $\mathcal{O}(h/e^2)$ peaks in ρ^{xx}, broadly consistent with the experimental observations in ref. 22. In the $T \to 0$ limit, the height of the ρ^{xx} peak at either transition is expected to saturate to a nonzero value while the width should decrease to zero as we described earlier. It would be interesting for future experiments to clarify these features of the resistance peaks. In principle, within the doped FQAH framework, there is also an alternative scenario in which the cheapest charged excitation for $\nu > \nu_2$ is simply the electron. If so, superconductivity can emerge from pairing of doped electrons on the Fermi surface, which leaves the background topological order intact. The transition temperature associated with this exotic SC* state, being exponentially suppressed in the inverse dopant density, is likely too small to account for the experimentally observed T_c.

Near the initial onset of superconductivity at $T = 0$ out of the anyon glass, we argued that the superconducting state is an Anomalous Vortex Glass with a random sprinkling of -2π and $+4\pi$ vortices with net zero vorticity. At $T > 0$, the AVG has a nonzero linear resistance which goes to zero only gradually as the temperature is decreased toward zero. This feature and the expected nonlinear response at small current bias are also seen in the experiments reported in ref. 22. Further studies are needed to establish whether these features are due to the AVG or have other mundane explanations.

An important future direction is a microscopic calculation of anyon energetics within models of tMoTe$_2$. It will be interesting to see whether "anyon bunching" of the kind reported in very recent calculations (24, 25) of Landau level FQH states happens in FQAH states found in models of tMoTe$_2$.[‖] However, even without numerics, existing data already provide some qualitative guidance. Given the sequence of Jain states observed near $\nu = 1/2$, it is natural to expect that the $\nu < 2/3$ side fits into the standard "composite fermion" framework (46). Since f_1 is the zero-field analogue of the composite fermion (see refs. 14, 47, and 48), it is reasonable to associate the nearest valence band with f_1. On the other hand, for $\nu > 2/3$, there is no a priori reason for the composite fermion framework to apply. Thus, our proposal of f_3 being the nearest conduction band becomes more plausible.

Tuning away from $D = 0$ modifies the anyon dispersion at $\nu = 2/3$. If there exists a critical D_c such that the nearest conduction band switches from f_3 to f_1 for $D > D_c$, then doping induces a fluid of $a_{1/3}$ anyons for both $\nu > 2/3$ and $\nu < 2/3$. This switching effect provides a potential explanation for the pair of RIQAH states observed in a range of displacement fields $15 \lesssim D \lesssim 30$ nV/nm on both sides of the FQAH plateau (22).

In order to test our hypothesis about anyon energetics, it will be important to have an experimental determination of the charge of the delocalizing anyon. This may be easier in the FQAH/anyon glass phase prior to the delocalization transition. Standard measurements (49–51) of the anyon charge successfully used in ordinary FQH systems are of course worth exploring in the FQAH context. An indirect route, specific to the lattice setting, is to look for local charge density modulations that are expected (52) to appear around each localized anyon (with short wavelength disorder) in a halo region at low dopant density. This is due to the close competition between FQAH and Charge Density Wave (CDW) phases in a clean system. Around each anyon, the FQAH is locally suppressed enabling the CDW to rear its head. These modulations may be measurable in

[#] In high quality tMoTe$_2$ devices, the density of charged point defects (which generate short-wavelength disorder) is about a factor of 100 smaller than the electron density. It is thus plausible that other sources of disorder (such as a random twist angle), which are only modulated at long wavelengths, play a dominant role.

[‖] See ref. 45 for a recent exact diagonalization (ED) study of anyon energetics in tMoTe$_2$. Importantly, this calculation only extracts the average of the quasiparticle gap Δ_q and the quasihole gap Δ_{-q} for each fractional $q > 0$. It remains to be seen whether Δ_q can be independently determined and compared with Δ_{nq} to test for anyon bunching.

Scanning Tunneling Microscopy experiments and their density can potentially yield the anyon charge (52).

Finally, our discussion of the transmutation of anyons of the FQAH into vortices of the SC could help test the basic validity of the anyonic mechanism of superconductivity. Following similar discussions in the context of the cuprates (31, 53, 54), vortex memory effects are expected when cycling an annulus between the superconductor and the FQAH state. Specifically $\pm h/2e$ vortices trapped in a hole inside the device would first disappear when the doping is tuned back into the insulator but would leave behind a threaded anyon. Upon cycling back into the SC, the anyon would nucleate the same vortex.

Note added-We are coordinating submission with ref. 55, where closely related results were obtained. Since the original posting of this paper on the arXiv, refs. 56 and 57 appeared on related topics, and ref. 45 on some pertinent microscopic calculations.

Data, Materials, and Software Availability. There are no data underlying this work.

ACKNOWLEDGMENTS. We thank Matthew Fisher, Tonghang Han, Eslam Khalaf, Tingxin Li, Pavel Nosov, Heonjoon Park, Nicolas Regnault, and Ashvin Vishwanath for discussions. Z.D.S. and T.S. are supported by NSF grant DMR-2206305.

Author affiliations: [a]Department of Physics, Massachusetts Institute of Technology, Cambridge, MA 02139

1. H. Park *et al*., Observation of fractionally quantized anomalous Hall effect. *Nature* **622**, 74–79 (2023).
2. Y. Zeng *et al*., Integer and fractional Chern insulators in twisted bilayer MoTe2. arXiv [Preprint] (2023). http://arxiv.org/abs/2305.00973 (Accessed 1 June 2025).
3. J. Cai *et al*., Signatures of fractional quantum anomalous Hall states in twisted $MoTe_2$. *Nature* **622**, 63–68 (2023).
4. F. Xu *et al*., Observation of integer and fractional quantum anomalous Hall effects in twisted bilayer $MoTe_2$. *Phys. Rev. X* **13**, 031037 (2023).
5. Z. Lu *et al*., Fractional quantum anomalous Hall effect in multilayer graphene. *Nature* **626**, 759–764 (2024).
6. Z. Lu *et al*., Extended quantum anomalous Hall states in graphene/hBN moiré superlattices. *Nature* **637**, 1090–1095 (2025).
7. H. L. Stormer, D. C. Tsui, A. C. Gossard, The fractional quantum Hall effect. *Rev. Mod. Phys.* **71**, S298–S305 (1999).
8. J. M. Leinaas, J. Myrheim, On the theory of identical particles. *Nuovo Cim. B* **37**, 1–23 (1977).
9. F. Wilczek, Magnetic flux, angular momentum, and statistics. *Phys. Rev. Lett.* **48**, 1144–1146 (1982).
10. F. Wilczek, Quantum mechanics of fractional-spin particles. *Phys. Rev. Lett.* **49**, 957–959 (1982).
11. R. B. Laughlin, Anomalous quantum Hall effect: An incompressible quantum fluid with fractionally charged excitations. *Phys. Rev. Lett.* **50**, 1395–1398 (1983).
12. B. I. Halperin, Statistics of quasiparticles and the hierarchy of fractional quantized Hall states. *Phys. Rev. Lett.* **52**, 1583–1586 (1984).
13. B. Huckestein, Scaling theory of the integer quantum Hall effect. *Rev. Mod. Phys.* **67**, 357–396 (1995).
14. Z. D. Shi, T. Senthil, Doping a fractional quantum anomalous Hall insulator. *Phys. Rev. X* **15**, 031069 (2025).
15. M. Kim, A. Timmel, L. Ju, X. G. Wen, Topological chiral superconductivity beyond pairing in a Fermi liquid. *Phys. Rev. B* **111**, 014508 (2025).
16. Z. Darius Shi, C. Zhang, T. Senthil, Doping lattice non-abelian quantum Hall states. arXiv [Preprint] (2025). http://arxiv.org/abs/2505.02893 (Accessed 1 June 2025).
17. R. B. Laughlin, Superconducting ground state of noninteracting particles obeying fractional statistics. *Phys. Rev. Lett.* **60**, 2677–2680 (1988).
18. A. L. Fetter, C. B. Hanna, R. B. Laughlin, Random-phase approximation in the fractional-statistics gas. *Phys. Rev. B* **39**, 9679–9681 (1989).
19. Y. H. Chen, F. Wilczek, E. Witten, B. I. Halperin, On anyon superconductivity. *Int. J. Mod. Phys. A* **4**, 3983 (1989).
20. D. H. Lee, M. P. A. Fisher, Anyon superconductivity and the fractional quantum Hall effect. *Phys. Rev. Lett.* **63**, 903–906 (1989).
21. S. Divic *et al*., Anyon superconductivity from topological criticality in a Hofstadter-Hubbard model. arXiv [Preprint] (2024). http://arxiv.org/abs/2410.18175 (Accessed 1 June 2025).
22. F. Xu *et al*., Signatures of unconventional superconductivity near reentrant and fractional quantum anomalous Hall insulators. arXiv [Preprint] (2025). http://arxiv.org/abs/2504.06972 (Accessed 1 June 2025).
23. R. Willett, J. P. Eisenstein, H. L. Stormer, A. C. Gossard, D. C. Tsui, Observation of an even-denominator quantum number in the fractional quantum Hall effect. *Phys. Rev. Lett.* **59**, 1776–1779 (1987).
24. Q. Xu, G. Ji, Y. Wang, H. Quang Trung, B. Yang, Dynamics of clusters of anyons in fractional quantum Hall fluids. arXiv [Preprint] (2025). http://arxiv.org/abs/2505.20257 (Accessed 1 June 2025).
25. M. Gattu, J. K. Jain, Molecular anyons in fractional quantum hall effect. arXiv [Preprint] (2025). https://arxiv.org/abs/2505.22782 (Accessed 10 June 2025).
26. M. P. A. Fisher, Vortex-glass superconductivity: A possible new phase in bulk high-t_c oxides. *Phys. Rev. Lett.* **62**, 1415–1418 (1989).
27. D. S. Fisher, M. P. A. Fisher, D. A. Huse, Thermal fluctuations, quenched disorder, phase transitions, and transport in type-II superconductors. *Phys. Rev. B* **43**, 130–159 (1991).
28. T. Senthil, S. Sachdev, M. Vojta, Fractionalized fermi liquids. *Phys. Rev. Lett.* **90**, 216403 (2003).
29. T. Senthil, M. Vojta, S. Sachdev, Weak magnetism and non-fermi liquids near heavy-fermion critical points. *Phys. Rev. B* **69**, 035111 (2004).
30. T. Senthil, M. P. A. Fisher, Z_2 gauge theory of electron fractionalization in strongly correlated systems. *Phys. Rev. B* **62**, 7850–7881 (2000).
31. T. Senthil, M. P. A. Fisher, Fractionalization in the cuprates: Detecting the topological order. *Phys. Rev. Lett.* **86**, 292–295 (2001).
32. M. P. A. Fisher, P. B. Weichman, G. Grinstein, D. S. Fisher, Boson localization and the superfluid-insulator transition. *Phys. Rev. B* **40**, 546–570 (1989).
33. M. P. A. Fisher, T. A. Tokuyasu, A. P. Young, Vortex variable-range-hopping resistivity in superconducting films. *Phys. Rev. Lett.* **66**, 2931–2934 (1991).
34. M. C. Cha, M. P. A. Fisher, S. M. Girvin, M. Wallin, A. P. Young, Universal conductivity of two-dimensional films at the superconductor-insulator transition. *Phys. Rev. B* **44**, 6883–6902 (1991).
35. K. Damle, S. Sachdev, Nonzero-temperature transport near quantum critical points. *Phys. Rev. B* **56**, 8714–8733 (1997).
36. S. Sachdev, Nonzero-temperature transport near fractional quantum Hall critical points. *Phys. Rev. B* **57**, 7157–7173 (1998).
37. M. P. A. Fisher, G. Grinstein, S. M. Girvin, Presence of quantum diffusion in two dimensions: Universal resistance at the superconductor-insulator transition. *Phys. Rev. Lett.* **64**, 587–590 (1990).
38. A. B. Harris, Effect of random defects on the critical behaviour of Ising models. *J. Phys. C Solid State Phys.* **7**, 1671 (1974).
39. J. T. Chayes, L. Chayes, D. S. Fisher, T. Spencer, Finite-size scaling and correlation lengths for disordered systems. *Phys. Rev. Lett.* **57**, 2999–3002 (1986).
40. X. Y. Song, Y. H. Zhang, T. Senthil, Phase transitions out of quantum Hall states in Moiré materials. *Phys. Rev. B* **109**, 085143 (2024).
41. C. L. Kane, M. P. A. Fisher, J. Polchinski, Randomness at the edge: Theory of quantum Hall transport at filling $\nu=2/3$. *Phys. Rev. Lett.* **72**, 4129–4132 (1994).
42. C. L. Kane, M. P. A. Fisher, Impurity scattering and transport of fractional quantum Hall edge states. *Phys. Rev. B* **51**, 13449–13466 (1995).
43. C. L. Kane, M. P. A. Fisher, Contacts and edge-state equilibration in the fractional quantum Hall effect. *Phys. Rev. B* **52**, 17393–17405 (1995).
44. C. Chamon, E. Fradkin, Distinct universal conductances in tunneling to quantum Hall states: The role of contacts. *Phys. Rev. B* **56**, 2012–2025 (1997).
45. M. Gonçalves *et al*., Spinless and spinful charge excitations in Moiré fractional Chern insulators. arXiv [Preprint] (2025). http://arxiv.org/abs/2506.05330 (Accessed 1 June 2025).
46. J. K. Jain, Composite-fermion approach for the fractional quantum Hall effect. *Phys. Rev. Lett.* **63**, 199–202 (1989).
47. H. Goldman, A. P. Reddy, N. Paul, L. Fu, Zero-field composite fermi liquid in twisted semiconductor bilayers. *Phys. Rev. Lett.* **131**, 136501 (2023).
48. J. Dong, J. Wang, P. J. Ledwith, A. Vishwanath, D. E. Parker, Composite fermi liquid at zero magnetic field in twisted $MoTe_2$. *Phys. Rev. Lett.* **131**, 136502 (2023).
49. L. Saminadayar, D. C. Glattli, Y. Jin, B. Etienne, Observation of the e/3 fractionally charged Laughlin quasiparticle. *Phys. Rev. Lett.* **79**, 2526–2529 (1997).
50. R de-Picciotto, *et al*., Direct observation of a fractional charge. *Phys. B Condens. Matter* **249**, 395–400 (1998).
51. J. Martin *et al*., Localization of fractionally charged quasi-particles. *Science* **305**, 980–984 (2004).
52. X. Y. Song, T. Senthil, Density wave halo around anyons in fractional quantum anomalous Hall states. *Phys. Rev. B* **110**, 085120 (2024).
53. T. Senthil, M. P. Fisher, Fractionalization, topological order, and cuprate superconductivity. *Phys. Rev. B* **63**, 134521 (2001).
54. D. Bonn *et al*., A limit on spin-charge separation in high-t_c superconductors from the absence of a vortex-memory effect. *Nature* **414**, 887–889 (2001).
55. P. A. Nosov, Z. Han, E. Khalaf, Anyon superconductivity and plateau transitions in doped fractional quantum anomalous Hall insulators. arXiv [Preprint] (2025). http://arxiv.org/abs/2506.02108 (Accessed 1 June 2025).
56. Y. H. Zhang, Holon metal, charge-density-wave and chiral superconductor from doping fractional Chern insulator and $SU(3)_1$ chiral spin liquid. arXiv [Preprint] (2025). http://arxiv.org/abs/2506.00110 (Accessed 1 June 2025).
57. F. Pichler, C. Kuhlenkamp, M. Knap, A. Vishwanath, Microscopic mechanism of anyon superconductivity emerging from fractional Chern insulators. arXiv [Preprint] (2025). https://arxiv.org/abs/2506.08000 (Accessed 10 June 2025).